Heat Transfer and Fluid Dynamics in Mercury-Water Spray Columns

R. D. PIERCE, O. E. DWYER, and J. J. MARTIN

University of Michigan, Ann Arbor, Michigan

Heat transfer and fluid dynamics were studied in columns in which hot mercury was sprayed into a rising stream of water. Volumetric and area heat transfer coefficients are presented which were found to be lower than those reported for heat transfer from fixed spheres.

It was observed that considerable water bypassed the stream of drops, while some surrounding the drops flowed downward. This behavior resulted in water temperatures at the base of the column which were considerably higher than the inlet water temperatures. Consequently the outlet mercury temperature did not approach the inlet water temperature as a limit. The very unconventional flow pattern of the water was unexpected and is believed to be an important factor in spray-column heat transfer and mass transfer kinetics.

Direct heat exchange between two immiscible liquids, in the absence of a separating wall, has the apparent advantage of rapid heat exchange and the possibilities of high-power densities and simple heat-exchanger design. If these should prove real, this kind of heat exchange would be attractive for liquid-fueled nuclear reactors. It was from this standpoint that the experimental work described in this article was undertaken.

It was suggested by workers at the Brookhaven National Laboratory some years ago that the liquid-metal–fuel reactor under development there might be cooled by the contacting of the molten uranium-bismuth fuel with a fused salt mixture. The purpose of this present study was to investigate the promise of direct liquid-liquid heat transfer for application to the LMFR.

This initial experimental work was simplified by the selection of mercury and water as representatives for bismuth and salt and by the employment of simple spray-column contactors. Heat transfer and fluid dynamics data obtained under such conditions can be used to indicate the potentialities of direct heat exchange in more complex equipment.

Heated mercury droplets were sprayed into the top of the columns, and water was introduced at the bottom. Columns of two different lengths and two different diameters and with several different spray nozzles were used.

Some heat transfer studies on spray columns dispersing organic solvents and water have been reported (*1, 3, 8*), but of course the physical properties of the organic phases were far different from those of liquid metals. A more nearly similar experiment involves the transfer of heat between metal spheres and fluids. Kramers(*5*) studied the transfer of heat from isolated steel spheres to flowing air, water, and oils. His data were correlated by the equation

$$N_{Nu} = 2.0 + 1.3(N_{Pr})^{0.15} + 0.66(N_{Pr})^{0.31}(N_{Re})^{0.50}$$

Williams (*9*) made an extensive study of the existing data for heat and mass transfer from single, stationary spheres and recommended the equation

$$N_{Nu} = 0.37(N_{Re})^{0.6}(N_{Pr})^{0.33}$$

for heat transfer over a range of Reynolds

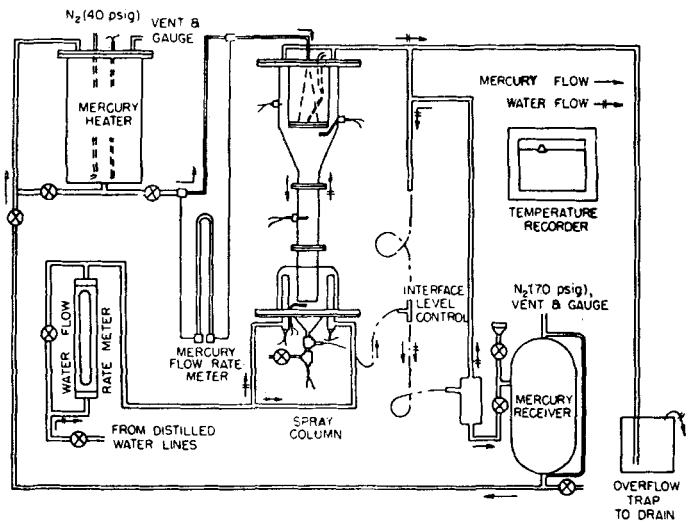

Fig. 1. Flow diagram.

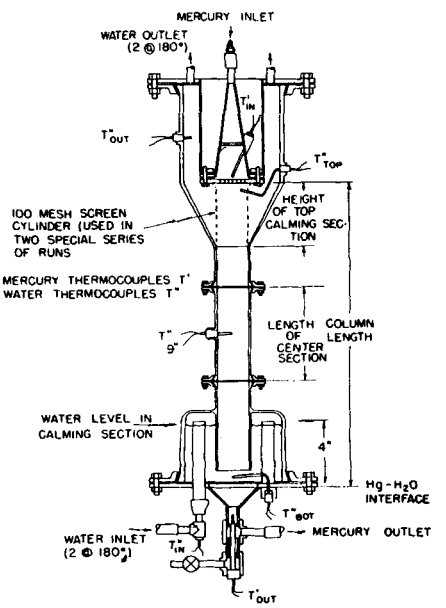

Fig. 2. Spray column.

R. D. Pierce is at Argonne National Laboratory, Lemont, Illinois, and O. E. Dwyer at Brookhaven National Laboratory, Upton, New York.

numbers between 2×10^2 and 2×10^5. Ranz (7) correlated a collection of data for both heat and mass transfer from single spheres over the Reynolds number range 1 to 10^5. He found that the heat transfer results under these conditions could be represented by

$$N_{Nu} = 2.0 + 0.60(N_{Pr})^{1/3}(N_{Re})^{1/2}$$

EXPERIMENTAL EQUIPMENT

Figure 1 is a flow sheet of the experimental equipment. Distilled water flowed *upward* through the column, while preheated mercury was sprayed from the top of the column and drained continuously from the bottom. In a single run 500 lb. of mercury could be passed through the column.

The columns used in this study, which are similar in design to the column used by Blanding and Elgin (2), are detailed in Figure 2. Six different columns were used, but the same steel end assemblies were used with each. The columns were fabricated from 1- and 2-in. I.D. Pyrex pipe. The enlarged ends of the columns were 6 in. I.D. to accommodate the end assemblies. The chief dimensions of the various columns are listed in Table 1.

Mercury, flowing at constant head from a pressurized header, entered the columns through a spray nozzle. The designs of the twelve fluorothene face plates which were used on this nozzle are listed in Table 2. The entire nozzle assembly was enclosed in a 4-in. cylinder which thermally isolated the nozzle from the water. The volume between the conical section and the cylinder was filled with asbestos insulation.

Mercury was collected at the bottom of the column in a conical pot, near the top of which the mercury-water interface was maintained. The pot and the fittings below it were also insulated.

Water entered the bottom calming section of the column through two vertical ½-in. pipes on opposite sides of the column. The water level in this section was maintained at the ends of these pipes. Water from the calming section flowed under a weir and then upward through the column, around the mercury nozzle, and out through two ½-in. pipes located on opposite sides of the annulus. In a few runs a cylinder made of 100-mesh stainless steel screening was placed at the top of the column as shown by the dotted lines in Figure 2

MEASUREMENTS

Temperatures

Temperatures were measured with 30-gauge copper-constantan thermocouples. The probes for these thermocouples were pieces of ⅛-in. O.D. stainless steel tubing, sealed at their inner ends. The thermocouple junctions, which extended about ⅛ in. beyond the insulation, were mounted in the tips of the probes with about ⅛ in. of soft solder.

The thermocouples were checked against a standard thermometer before being placed in the equipment; however several were also calibrated in place, since they were in electrical contact with the equipment. All thermocouples were connected to a 16-point Brown Electronik Recorder with a range of 60° to 220°F.

Figure 2 shows the locations of the thermocouples in the column. Mercury thermocouples were located inside the nozzle and below the collecting pot. Inlet water temperatures were measured in both inlet pipes, the thermocouple that measured the temperature of the water at the bottom of the column being located ½ in. above the mercury interface and midway between the center line and the wall of the column. The water temperature at the top of the column was measured with a thermocouple located outside the stream of mercury drops and 1 in. below the mercury nozzle, with another thermocouple approximately 2 in. above the face of the mercury nozzle. Water temperatures were also measured in the middle of the center sections, when they were used. The three thermocouples which entered the column through the glass walls extended through rubber stoppers; the others entered the column through packing glands or drilled pipe plugs.

A differential-thermocouple pair was used to measure the difference in temperature between the mercury and water at the bottom of the column. A Rubicon high-precision potentiometer was used with this pair. When the flow of mercury was suddenly stopped, the differential couples indicated that the temperature difference could be determined from the Brown recorder readings with an uncertainty of only 0.1°F. However under normal operating conditions the water-temperature variations were such that satisfactory readings could not be obtained with the differential thermo-

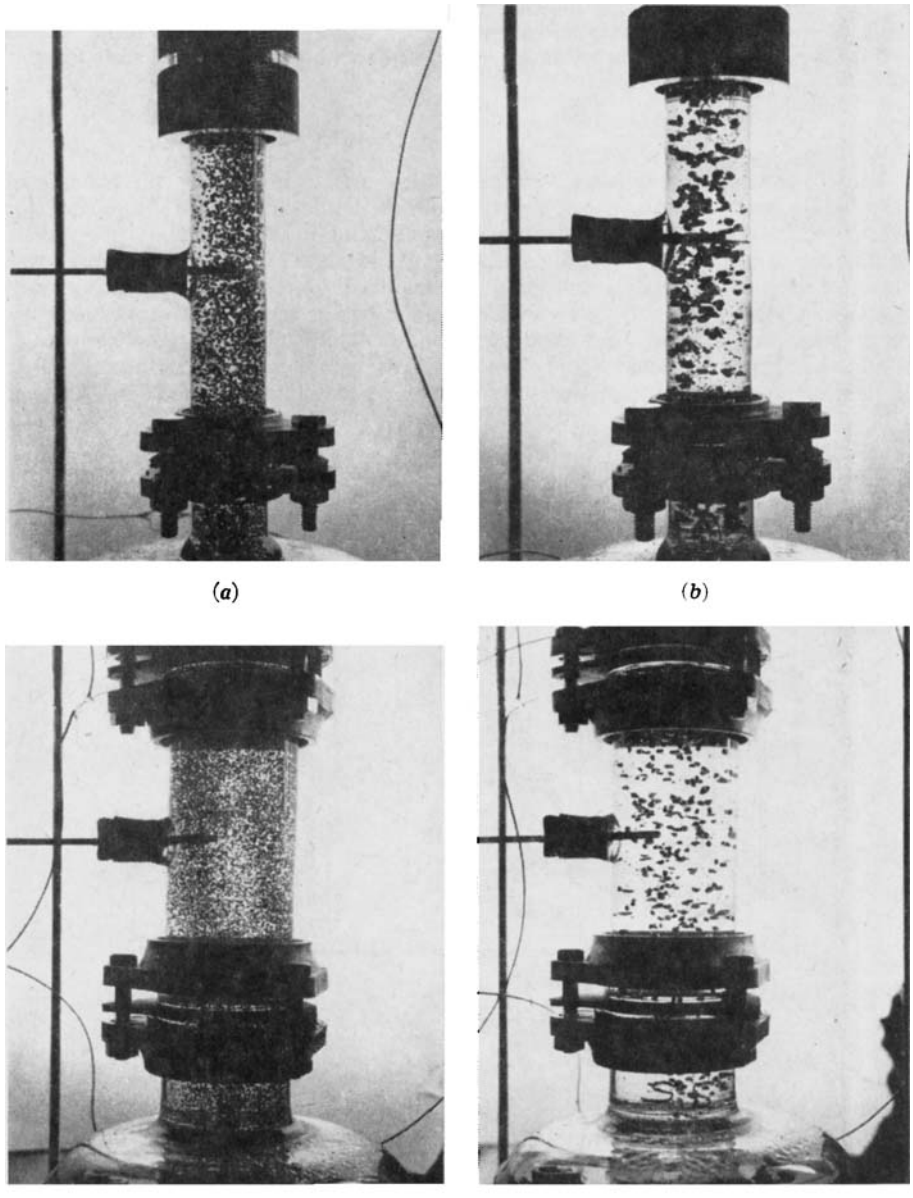

Fig. 3. Photographs of center section of column showing relative drop sizes for different nozzle designs: (*a*) average drop size 0.042 in., column 1 in. in diameter by 19.4 in. long, nozzle 21 holes by 0.031 in. in diameter; (*b*) average drop size 0.115 in., column 1 in. in diameter by 19.4 in. long, nozzle 5 holes by 0.089 in. in diameter; (*c*) average drop size 0.027 in., column 2 in. in diameter by 19.4 in. long, nozzle 29 holes by 0.032 in. in diameter; (*d*) average drop size 0.10 in., column 2 in. in diameter by 19.4 in. long, nozzle 9 holes by 0.070 in. in diameter.

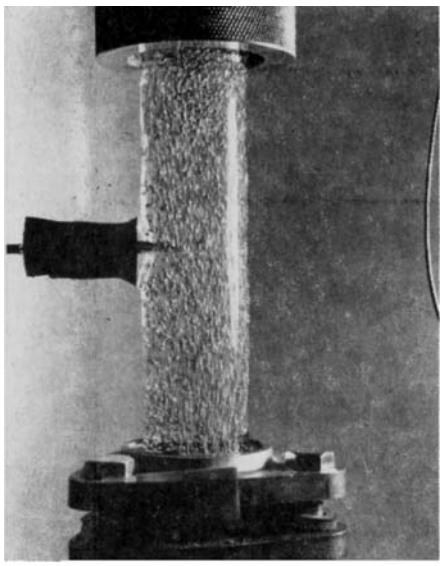

(a)

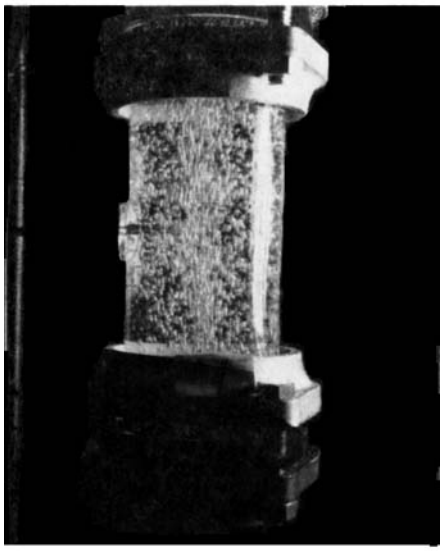

(b)

Fig. 4. Photographs of center section of column showing streaks due to velocity effect: (a) average drop size 0.042 in., column 1 in. in diameter by 19.4 in. long nozzle 21 holes by 0.031 in. in diameter; (b) average drop size 0.027 in., column 2 in. in diameter by 19.4 in. long, nozzle 29 holes by 0.032 in. in diameter.

couples and the manually operated potentiometer. Since the 16-point recorder could also be used to indicate continuously, but not record, any one of the points, the water temperature was often determined from periodic observations of the indicated temperature. Each day before the equipment was operated, the readings of the two thermocouples at the bottom of the column were checked to see that they were the same.

Water Flow Rate

The water flow rate was measured with a Fischer and Porter Flowrator, having a range of 0.06 to 0.6 gal./min. The Flowrator calibration was checked periodically and found to be accurate to within 1%. The water flow rate did not fluctuate more than 0.01 gal /min. at a flow rate of 0.6 gal./min.

Mercury Flow Rate

Mercury flow rates were indicated by an orifice flowmeter which was used to set and maintain a steady flow; however the time-volume relationship for the mercury collected in the receiver was used to determine the actual flow rate. Over the range used, the volume of the receiver was known to within 1%. Because of movement of mercury in the tank, temperature variations in the mercury, and uncertainties in reading the level indicator, the flow rates were estimated to be uncertain by approximately 2%.

Drop Sizes

Figures 3*a* through 3*d* are prints of a few of the photographs which were used to determine drop size. Mercury drops were photographed at a minimum of four mercury rates in each column and with each nozzle. These pictures were not taken during actual heat transfer runs but were made under similar temperature conditions.

Owing to distortion by the curved walls of the columns only vertical dimensions of the drop images were measured. The measurements were made on images which had been projected to about thirty times actual size. Between thirty and ninety measurements were made from each picture, depending on the total number of drops and the variation in their sizes. Under some conditions a number of very small drops were observed in the columns. These drops, which usually represented less than 1% of the mercury in the column and which appeared to remain fluidized, were not measured.

The maximum variation of apparent drop size with distance from the camera was 5% with the 2-in. columns and 3% with the 1-in. columns. This effect tends to be self-compensating when average dimensions are determined. Drop-size measurements were limited by the sharpness of the images. This caused an uncertainty of about 10% for the smallest drops and about 5% for the larger ones. The drop sizes produced by the five- and the one-hole nozzles are uncertain because of the irregular shapes of the larger drops.

Drop Velocities

Drop velocities also were obtained from photographs. The pictures were taken at an exposure time of 0.0033 ± 0.0001 sec. The drop images were elongated as a result of their motion. A small light reflection or high light was produced on one side of each drop, and the vertical length of these high lights was measured to determine drop velocities. Sample pictures are shown in Figure 4.

The velocity pictures were taken during special runs which duplicated the temperature conditions encountered during the heat transfer runs. These pictures were taken in the 19 3/8-in. columns only, but the results are assumed to apply equally well to the shorter columns. A minimum of four mercury rates were photographed with each nozzle. Between 100 and 250 measurements were made from each picture depending on the number of drops in the column. These measurements were taken from images projected to about thirty times actual size. The shutter speed was checked after every

Table 1. Spray-Column Dimensions

Diameter, in.	Length, in.	Length of center section, in.	Height of top calming section, in.
1	13¼	omitted	3¾
1 (Special)	13¼	omitted	3¾ (with 1 in. diam. 100 mesh screen cylinder)
1	19⅜	6	3¾
2	13¼	omitted	2¾
2	19⅜	6	2¾
2 (Special)	19⅜	omitted	6

Table 2. Mercury-Nozzle Details (Fluorothene Plates, ¼ in. Thick and 4 in. Diam.)

Number of holes	Diameter of holes, in.	Layout of holes, in.
With 1-in.-diameter columns		
73	0.0225	3/32 sq. pitch
21	0.031	3/16 sq. pitch
21	0.042	3/16 sq. pitch
16	0.046	3/16 sq. pitch
12	0.055	¼ sq. pitch
9	0.063	¼ sq. pitch
5	0.089	5/16 sq. pitch
1	0.189	centered
With 2-in.-diameter columns		
113	0.016	5/32 sq. pitch
29	0.032	¼ sq. pitch
64	0.046	3/16 sq. pitch
9	0.070	½ sq. pitch

series with the aid of a photoelectric cell and a cathode-ray oscilloscope.

The lengths of the high lights could not be measured more accurately than by about ±7%, because the edges of the images were not sharp. Variations in the distance between the camera and the drops made the magnification factors uncertain by as much as 5% for isolated drops, but this effect could be considered to cancel itself when average velocities were determined.

Water-Phase Movement

To study movements of the water phase during the operation of the columns, the authors injected dye in the water at one of four different locations: in the inlet water ahead of the column, in the outlet water at the position normally occupied by the outlet water thermocouple, in the top calming section, and in the middle of the column. A Fastex motion picture camera was used to record some of the observations. Most of the motion pictures were taken at a film speed of 1,500 frames/sec.

EXPERIMENTAL RESULTS

Heat Transfer Data

Typical temperature data are shown on Figure 5, the complete experimental data being presented in reference *6*.

Temperatures were recorded after

steady state conditions had been attained. The temperature profiles indicated on Figure 5 are qualitative, because the mercury temperature was determined only at inlet and outlet conditions and the water temperature only at the column ends except in the longer columns. The marked discontinuity in the temperature of the water entering the column was noted in all the runs.

Heat Transfer Calculations

Logarithmic-mean volumetric heat transfer coefficients were calculated by

$$Ua = \frac{q_{Hg}}{V\Delta T_{LM}} \tag{1}$$

where

$$\Delta T_{LM} = \frac{(T_{Hg})_{IN} - (T_{H_2O})_{TOP} - (T_{Hg})_{OUT} + (T_{H_2O})_{BOT}}{\ln \dfrac{(T_{Hg})_{IN} - (T_{H_2O})_{TOP}}{(T_{Hg})_{OUT} - (T_{H_2O})_{BOT}}}$$

Drop-velocity and drop-size data were used to determine mercury holdup, H, and area factors, a. The volumetric holdup is defined by

$$H = \frac{R}{\rho_{Hg}\bar{v}_H} \tag{2}$$

The following expression was used simultaneously with Equation (2) to determine $\bar{v}_H$ and H:

$$\bar{v}_H = \bar{v}_0 - \frac{W}{1 - H} \tag{3}$$

Equation (3) says that the relative velocity of the mercury droplets throughout the column is independent of the water flow rate. This is not necessarily true, but since the water-velocity term in Equation (3) was usually less than one tenth as large as $\bar{v}_0$, the effect on $\bar{v}_H$ should be small.

Area factors were determined from mercury holdup by Equation (5)

$$a = \frac{\sum_{n=1}^{n=n_T} n\pi d^2}{V} \tag{4}$$

$$= \frac{H}{\left(\frac{\pi d^3}{6}\right)}(\overline{\pi d^2}) = \frac{6H}{\frac{(\overline{d^3})}{(\overline{d^2})}} \tag{5}$$

Heat transfer coefficients on an area basis were determined by the division of the volumetric coefficients by the factor a.

DISCUSSION OF RESULTS

Heat Transfer

Three quantities, q, V, and ΔT, were used in the calculation of the volumetric heat transfer coefficients. The heat rate was calculated from the mercury data. This value could not be checked with the water data because of heat losses from the system. The water energy gain averaged about 7% lower than the energy loss for the mercury, but at the highest water temperatures the water heat values ran between 15 and 20% low. The greatest possibility of error in the values of q_{Hg} is that the mercury passing through the outside holes in the nozzles might have been cooler than the mercury at the center where the temperature was measured. Since the nozzle assembly was insulated and heat transfer data were taken at steady state, the errors in the heat term are probably small.

The temperature potential ΔT_{LM} is the most uncertain quantity. The temperature difference at the bottom of the column ΔT_{BOT} was difficult to measure because fluctuations in $(T_{H_2O})_{BOT}$ were large compared with ΔT_{BOT}. The mean deviation in ΔT_{BOT} for most runs was about 50%. Under some conditions the mean deviation was greater than 100%, but generally no coefficients were determined from these runs.

The use of logarithmic mean temperature difference in the heat transfer calculations is valid only when the integral $\int_0^q (dq/\Delta T)$ is equal to $q/\Delta T_{LM}$. This quality exists when ΔT is a linear function of q. In these experiments the mercury temperature is linear with the heat transferred. Since water temperatures are affected by recirculation and heat losses, their relationship to q is not necessarily linear, but they appear to be approximately linear with the heat transferred. If both the mercury and water temperatures are linear with q, the temperature difference is also linear with q.

The accuracy of the area heat transfer coefficients is also dependent upon the drop velocity and drop size as well as the heat transfer data. Examination of the photographs indicated that drop sizes and velocities for the same operating condition agreed to within 10%. Since the area factors are inversely proportional to velocity and drop diameter [Equations (2) and (5)], a given percentage error in either v_H or d would result in the same percentage error in the heat transfer coefficient.

If the resistance to heat transfer is assumed to be principally in the water phase, the variables affecting the heat transfer coefficient can be treated by dimensional analysis. Equation (6) relates the variables which are assumed to affect the heat transfer coefficients

$$N_{Nu} = f\left(N_{Re}, N_{Pr}, \frac{D}{d}, \frac{L}{d}, H, \phi\right) \tag{6}$$

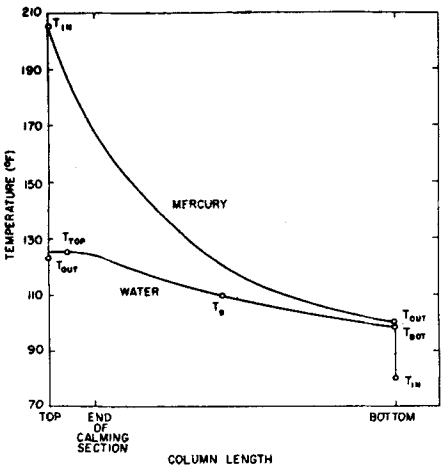

Fig. 5. Apparent temperature profiles in column.

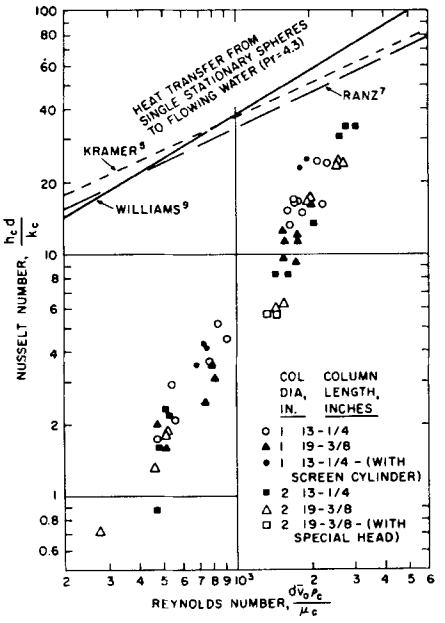

Fig. 6. Nusselt number vs. Reynolds number.

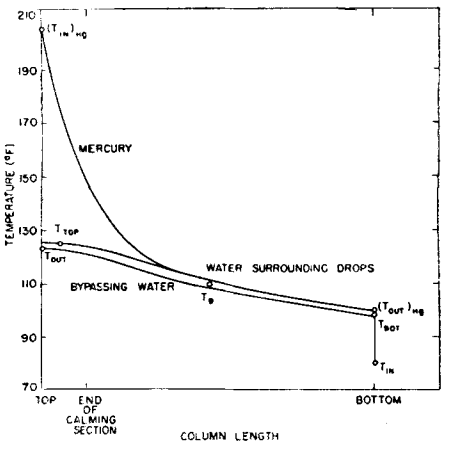

Fig. 7. Probable temperature profiles in column.

TABLE 3. SAMPLE RESULTS

Hg flow rate, lb./(min.)(sq. ft.)	H_2O flow rate, gal./(min.)(sq. ft.)	$\bar{d}^3/\bar{d}^2$, in.	v_0, ft./sec.	Pr	Re	$\phi \times 10^{-4}$	H, vol. %	a, sq. ft./cu. ft.	$Ua \times 10^{-3}$, B.t.u./(hr.)(cu. ft.)(°F.)	U (= h_{H_2O}), B.t.u./(hr.)(sq. ft.)(°F.)	Nu
	Column: 1 in. diam. × 13-¼ in. long Nozzle: 21 holes × 0.031 in. diam.										
2,000	54.8	0.045	1.65	4.4	830	43.1	2.51	38.5	19.3	502	5.2
3,500	36.6	0.043	1.6	3.7	950	49.5	4.43	71.8	31.5	439	4.3
3,500	54.8	0.043	1.6	3.9	900	44.6	4.54	73.7	33.8	459	4.5
3,500	73.2	0.043	1.6	4.0	880	42.4	4.67	75.7	35.6	470	4.6
3,500	91.4	0.043	1.6	4.3	810	36.7	4.80	77.8	35.6	458	4.5
3,500	109.8	0.043	1.6	4.7	750	32.4	4.93	80.0	40.3	504	6.9
5,000	54.8	0.040	1.55	3.8	770	35.8	7.08	121.4	48.3	399	3.6
	(Special runs using 100 mesh screen cylinder in column)										
2,000	54.8	0.045	1.65	5.1	730	33.2	2.51	38.5	16.0	416	4.3
3,500	54.8	0.043	1.55	4.8	750	31.3	4.54	73.7	29.8	405	4.2
5,000	54.8	0.040	1.55	4.4	680	27.6	7.08	121.4	46.7	386	3.5
	Column: 1 in. diam. × 13-¼ in. long Nozzle: 9 holes × 0.063 in. diam.										
3,500	36.6	0.094	2.1	3.7	2230	507	3.43	25.8	30.1	1170	24.8
3,500	54.8	0.094	2.1	3.9	2110	455	3.50	26.3	30.0	1140	24.2
3,500	73.2	0.094	2.1	3.9	2110	455	3.57	26.8	31.2	1160	24.6
3,500	91.4	0.094	2.1	3.8	2170	480	3.65	27.4	31.4	1150	24.4
3,500	109.8	0.094	2.1	4.0	2060	433	3.73	28.0	32.1	1150	24.4
5,500	54.8	0.094	2.1	3.6	2330	550	5.50	41.3	47.2	1110	23.8
	(Special runs using mesh screen cylinder in column)										
3,500	54.8	0.094	2.1	4.7	1800	333	3.50	26.3	28.2	1070	22.8
4,500	54.8	0.094	2.1	4.3	1930	486	4.50	33.8	39.0	1160	24.7
	Columns: 1 in. diam. × 19-⅜ in. long Nozzle: 21 holes × 0.031 in. diam.										
2,000	54.8	0.045	1.65	4.7	780	37.9	2.51	38.5	13.5	347	3.6
3,500	54.8	0.043	1.6	4.4	810	36.5	4.54	73.7	23.3	316	3.1
5,000	54.8	0.040	1.55	4.1	740	32.4	7.09	121.4	33.4	275	2.5
	Column: 2 in. diam. × 13-¼ in. long Nozzle: 29 holes × 0.032 in. diam.										
900	18.4	0.048	2.6	4.4	1420	49.2	0.73	10.7	8.13	762	8.3
1,400	18.4	0.048	2.6	3.9	1600	62.4	1.14	16.7	12.65	760	8.3
	Column: 2 in. diam. × 19-⅜ in. long Nozzle: 29 holes × 0.032 in. diam.										
900	18.4	0.048	2.6	4.4	1440	51.2	0.73	10.7	5.9	553	6.0
1,400	18.4	0.048	2.6	4.0	1560	58.7	1.14	16.7	9.8	587	6.4
	Column: 2 in. diam. × 19-⅜ in. long (with special top head) Nozzle: 29 holes × 0.032 in. diam.										
900	18.4	0.048	2.6	4.8	1310	42.0	0.73	10.7	5.6	523	5.7
1,400	18.4	0.048	2.6	4.4	1440	50.0	1.14	10.7	8.7	521	5.7

Some values of the dimensionless groups in Equation (6) are listed in Table 3. The physical properties of water at a temperature midway between T_{TOP} and T_{BOT} were used to evaluate these groups. The mean slip velocity could not be measured but was assumed to be equal to the average drop velocity at zero water rate. The nature of the relationship between the dimensionless groups of Equation (6) could not be determined, however, because the drop diameter, which appears in nearly all the groups, was the only variable which could be independently controlled.

Reynolds and Nusselt numbers from all the columns and nozzles are plotted in Figure 6 along with the correlations of Kramers (*4*), Ranz (*6*), and Williams (*8*) for heat transfer from single stationary spheres. The Prandtl number for the three correlation lines in the figure was 4.3, while that for the data points varied from about 3.7 to 5.0. The data on this plot indicate that the heat transfer coefficients for the 19-in. columns are about 20% lower than those in the 13-in. columns. The effects of column diameter, height of top calming section, and mixing in the top section on these coefficients appear slight.

Heat transfer results at varying water rates (Table 3) indicate that both volumetric and area heat transfer coefficients increase only slightly with increased water rates.

Water-Phase Dynamics

For nearly every heat transfer run the temperature difference $[(T_{H_2O})_{BOT} - (T_{H_2O})_{IN}]$ was much greater than the temperature difference $[(T_{Hg})_{OUT} - (T_{H_2O})_{BOT}]$, which indicates that the heat transfer coefficients were a relatively minor factor influencing the total heat transferred to the incoming water.

The unexpectedly high values of $(T_{H_2O})_{BOT}$ were not due to the fact that

TABLE 4. MAXIMUM WATER VELOCITY IN THE CENTER SECTION OF THE 1-IN-DIAMETER × 19⅜-IN.-LONG SPRAY COLUMN

Net Water Flow Rate:
0.12 cu. ft./(sq. ft.)(sec.)
54.8 gal./(min.)(sq. ft.)

Drop size, in	Mercury rate, lb./(sq. ft.)(min.)	Velocity, ft./sec. Up	Down
0.042	2,600	1.6	0.2
0.042	4,600	2.5	0.3
0.042	5,700	2.0	1.6
0.092	2,600	1.8	0.4
0.092	4,600	2.0	0.6
0.092	5,700	2.0	2.0

the thermocouple measuring the temperature of the water at the bottom of the column was overheated by contact with the falling mercury. This was demonstrated by the variation of the location of the thermocouple.

The effects of column diameter and variation in height of top calming section on the heat transfer coefficients were negligible. The data taken in the 1-in. column with the 100-mesh screen cylinder below the mercury nozzle showed larger temperature discontinuities than data taken without the screen. Probably the increase in the temperature T_{BOT} was an indirect result of an increase in the water temperature under the mercury nozzle caused by the reduced circulation in this region. Since the thermocouple which measured T_{TOP} was located just outside the screen, the true top water temperature was probably slightly higher than that measured. The location of this thermocouple, outside the mercury stream, was shown to be satisfactory when the screen was not present but was not verified for the runs with the screen.

The sharp rise in water temperature at the water inlet was caused by the mixing produced by turbulence in and internal recirculation of the water phase. This was evident in both the motion pictures and in the drop velocity pictures. The principal upward flow of water bypassed the falling mercury drops. This rising stream of water continually shifted around the column but generally passed along one side opposite the flowing mercury. Thus two countercurrent streams of water flowed in the columns. Table 4 lists maximum upward and downward water velocities determined from six of the motion pictures. All the water in the columns was observed to undergo considerable recirculation during the flow of mercury Even water near the inlet and outlet water pipes recirculated to and from the vicinity of the drops. The pictures of dye movements showed relatively little mixing between the rising and falling streams of water. Since horizontal mixing appears slight, an appreciable resistance to heat transfer might exist between water flowing concurrently with the mercury drops and that bypassing them. Three heat transfer observations indicated that this resistance might be important in the mercury-water columns:

1. Over-all heat transfer coefficients decreased with increased column length. This would result if the heat transfer resistance between the countercurrent water streams was relatively large, so that a large portion of the total heat transfer occurred at the ends of the columns were the contact was more complete.

2. Variation in volumetric heat transfer coefficients with drop size is less than would be expected as a result of the increased mercury surface area.

3. Temperature discontinuities which were observed in the 13- and 19-in. columns were almost identical.

If heat transfer to the bypassing water were an important mechanism in these experiments, the mercury temperature profile presented on Figure 5 would not be correct, because the mercury temperature would drop more rapidly. The average water-temperature profile would be the same, because it was average water temperatures that were measured. Figure 7 may more nearly represent the true temperature profiles, which were obtained by assuming the double water profiles shown and estimating the mercury profile from the heat transfer data for fixed spheres.

CONCLUSIONS

Extremely rapid heat transfer was experienced between the dispersed phases in the mercury-water columns. The major transfer resistance was within the bulk of the water phase. Heat transfer results did not vary appreciably with minor changes in column design nor between 1-and 2-in.-diam. columns, but the column efficiencies decreased markedly with increased column length.

This study has illustrated that flow patterns can greatly limit the efficiency of liquid-liquid spray columns. The columns were found to operate with a stream of water flowing with the falling mercury drops and with the principal upward flow of water bypassing the drops. This flow pattern produced a discontinuous rise in the temperature of the water entering the columns. The sharp change in water temperature prevented the outlet mercury temperatures from approaching the inlet water temperatures as a limit. Similar phenomena have been observed recently in organic-water, mass transfer systems (*4*), but the effect has been overlooked in most spray column studies.

ACKNOWLEDGMENT

This paper is based on work supported by the U. S. Atomic Energy Commission and carried out by R. D. Pierce, the principal investigator, as a thesis for the Doctor of Philosophy degree from the University of Michigan, Ann Arbor, Michigan.

NOTATION

a = surface area of drops per unit column volume, sq. ft./cu. ft.
c = specific heat, B.t.u./(lb.)(°F.)
D = diameter of column, ft.
d = diameter of drop or particle, ft.
f = operator signifying function of, dimensionless
g = acceleration due to force of gravity, ft./sec.^{2}
H = volumetric fraction holdup of discontinuous phase, cu. ft./cu. ft.
h = heat transfer coefficient, B.t.u./(hr.)(sq. ft./°F.)
k = thermal conductivity, B.t.u./hr. sq. ft. (°F./ft.)
L = column length, ft.
N = number of drops entering column per unit time, sec.$^{-1}$
N_{Nu} = Nusselt number, $h_c d/k_c$, dimensionless
n = number of particular drop in column or number of drops in the column, dimensionless
N_{Pr} = Prandtl number, $(c\mu/k)_c$, dimensionless
q = rate of heat transfer, B.t.u./hr.
R = mass rate of flow mercury per unit area, lb./(sq. ft.)(sec.)
N_{Re} = Reynolds number, $dv_s\rho_c/\mu_c$, dimensionless
S = inside sectional area of empty column, sq. ft.
T = Temperature, °F.
U = overall heat transfer coefficient, B.t.u./(hr.)(sq. ft./°F.)
V = effective column volume, cu. ft.
v = velocity, ft./sec.
W = volume rate of flow of water per unit area, cu. ft./(sq. ft.)(sec.)
μ = coefficient of viscosity, lb./(ft.)(sec.)
ρ = density, lb./cu. ft.
ϕ = $d^3g\rho_c(\rho_d - \rho_c)/\mu_c^2$, dimensionless

Bar over a symbol = arithmetic average value

Subscripts

BOT = bottom of column
c = continuous phase
d = dispersed phase
H = holdup
LM = logarithmic mean value
n = particular drop
o = zero water flow rate
s = slip or contact velocity
T = total

LITERATURE CITED

1. Allen, H. D., W. A. Kline, E. A. Lawrence, C. J. Arrowsmith, and C. Marsel *Chem. Eng. Progr.*, **43**, 459 (1947).
2. Blanding, F. H., and J. C. Elgin, *Trans. Amer. Inst. Chem. Eng.*, **38**, 305 (1942).
3. Garwin, Leo, and B. D. Smith, *Chem. Eng. Progr.*, **49**, 591 (1953).
4. Geankoplis, C. J., P. L. Wells, and E. L. Hawk, *Ind. Eng. Chem.*, **43**, 1848 (1951).
5. Kramers, H., *Physica*, **12**, 2–3 61 (1946).
6. Pierce, R. D., Ph.D. thesis, Univ. of Mich., Ann Arbor (1954).
7. Ranz, W. E., *Chem. Eng. Progr.*, **48**, 247 (1942).
8. Rosenthal, Howard, master's thesis, New York Univ., New York (1949).
9. Williams, G. G., Ph.D. thesis, Mass. Inst. of Tech., Cambridge (1942).

Presented at A.I.Ch.E. Detroit Meeting. Manuscript received October, 1958; revision received October 17, 1958; paper accepted October 18, 1958.